Oxidized and reduced sulfur observed by the Sample Analysis at Mars (SAM) instrument suite on the Curiosity rover within the Glen Torridon region at Gale crater, Mars

Gregory M Wong, H B Franz, J V Clark, A C Mcadam, J M T Lewis, Maëva Millan, D W Ming, F. Gomez, B. Clark, Jennifer Eigenbrode, et al.

▶ **To cite this version:**

Gregory M Wong, H B Franz, J V Clark, A C Mcadam, J M T Lewis, et al.. Oxidized and reduced sulfur observed by the Sample Analysis at Mars (SAM) instrument suite on the Curiosity rover within the Glen Torridon region at Gale crater, Mars. Journal of Geophysical Research. Planets, 2021, 6 (1), pp.129-140. 10.1029/2021je007084 . hal-03754907

HAL Id: hal-03754907
https://hal.science/hal-03754907

Submitted on 20 Aug 2022

HAL is a multi-disciplinary open access archive for the deposit and dissemination of scientific research documents, whether they are published or not. The documents may come from teaching and research institutions in France or abroad, or from public or private research centers.

L'archive ouverte pluridisciplinaire **HAL**, est destinée au dépôt et à la diffusion de documents scientifiques de niveau recherche, publiés ou non, émanant des établissements d'enseignement et de recherche français ou étrangers, des laboratoires publics ou privés.

Check for updates

Accepted Article

Oxidized and reduced sulfur observed by the Sample Analysis at Mars (SAM) instrument suite on the Curiosity rover within the Glen Torridon region at Gale crater, Mars

G. M. Wong[1], H. B. Franz[2], J. V. Clark[3], A. C. McAdam[2], J. M. T. Lewis[2,4,5], M. Millan[2,6] D. W. Ming[7], F. Gomez[8], B. Clark[9], J. L. Eigenbrode[2], R. Navarro-González[10,†], C. H. House[1,11]

[1]Department of Geosciences, The Pennsylvania State University, University Park, PA, USA. [2]NASA Goddard Space Flight Center, Greenbelt, MD, USA. [3]GeoControls Systems – Jacobs JETS Contract at NASA Johnson Space Center, Houston, TX, USA. [4]Department of Physics and Astronomy, Howard University, Washington, DC, USA. [5]Center for Research and Exploration in Space Science and Technology, NASA GSFC, Greenbelt, MD, USA. [6]Department of Biology, Georgetown University, Washington, DC, USA. [7]NASA Johnson Space Center, Houston, TX, USA. [8]Centro de Astrobiologia (CSIC- INTA), Torrejón de Ardoz, Madrid, Spain. [9]Space Science Institute, Boulder, CO, USA. [10]Instituto de Ciencias Nucleares, Universidad Nacional Autónoma de México, Ciudad Universitaria, Ciudad de México, Mexico. [11]Earth and Environmental Systems Institute, The Pennsylvania State University, University Park, PA 16802, USA.

Corresponding author: Gregory Wong (gkw5061@psu.edu)

†Deceased January 28, 2021

Key Points:

- The *Curiosity* rover investigated sulfur from the clay-bearing Glen Torridon region with the Sample Analysis at Mars instrument suite
- Multiple analyses (evolved gases, isotopes, comparative laboratory research) were used to determine whether sulfur was oxidized or reduced
- The samples mostly contained oxidized sulfur, but two had results consistent with reduced sulfur, which has implications for habitability

This article has been accepted for publication and undergone full peer review but has not been through the copyediting, typesetting, pagination and proofreading process, which may lead to differences between this version and the Version of Record. Please cite this article as doi: 10.1029/2021JE007084.

This article is protected by copyright. All rights reserved.

Abstract

The Mars Science Laboratory (MSL) *Curiosity* rover has been assessing the habitability and geologic history of Gale crater, Mars since landing in 2012. One of the primary objectives of the mission was to investigate a clay-bearing unit identified using orbital spectral data, designated the Glen Torridon (GT) region. This region was of particular interest because of its elevated abundance of clay minerals that may have preserved geochemical evidence of ancient habitable environments. The *Curiosity* rover explored the GT region for ~750 sols and analyzed eight drilled samples with the Sample Analysis at Mars (SAM) instrument suite using evolved gas analysis-mass spectrometry. Evolved sulfur-bearing gases provided insight about the composition of sulfur-containing compounds in Martian samples. Evolved gases were analyzed by three methods to understand the oxidation state of sulfur in the samples: (1) SO_2 evolution temperature, (2) quadratic discriminant analysis comparing SAM data to SAM-like laboratory investigations, and (3) sulfur isotope values from evolved $^{34}SO_2/^{32}SO_2$. The results of these three methods were consistent with the majority of sulfur in the GT region being in an oxidized state, but two of the eight samples analyzed by SAM were consistent with the presence of small amounts of reduced sulfur. The oxidized and reduced sulfur could have a variety of sources and represents a nonequilibrium assemblage that could have supported putative ancient chemolithotrophic metabolisms.

Plain Language Summary

The Mars Science Laboratory (MSL) *Curiosity* rover has been searching for ancient habitable environments in Gale crater, Mars, since 2012. Orbital data indicated the presence of a clay mineral-rich region along the rover's traverse, which could have preserved geochemical evidence of ancient habitable environments. MSL drilled several samples from this region, now called the Glen Torridon region, and analyzed the samples' chemistry. The work here describes analyses of the sulfur chemistry from these samples as determined from the Sample Analysis at Mars (SAM) instrument suite. The chemical state of sulfur in the samples was determined by a combination of SAM data and comparative laboratory investigations. While most of the sulfur in this clay-bearing region was consistent with the presence of sulfate (SO_4^{2-}), two samples were consistent with the presence of small amounts of sulfide (S^{2-}). The presence of both sulfide and sulfate could have supported the energy requirements of ancient microorganisms if they were present.

Accepted Article

This article is protected by copyright. All rights reserved.

1 Introduction

1.1 Geologic Context of Gale Crater and the Glen Torridon Region

The Mars Science Laboratory (MSL) *Curiosity* rover has been exploring Gale crater, Mars, since August 2012 to assess the region's geologic history, present environment, and potential evidence of past habitability (Grotzinger et al., 2012, 2015). Gale crater, a ~155 km diameter impact crater of Noachian age, is located near the Martian equator at the crustal dichotomy and features ~5 km of exposed stratigraphy that forms a central mound called Aeolis Mons, informally referred to as Mt. Sharp (Grotzinger & Milliken, 2012; Wray, 2013). Spectral data from orbiters were used to identify key targets within Gale crater for *in-situ* exploration by *Curiosity*. For example, the Thermal Emission Imaging System (THEMIS) on board the Mars Odyssey orbiter identified a high thermal inertia unit (representative of well-cemented sedimentary rocks) on the crater floor. Similarly, the Compact Reconnaissance Imaging Spectrometer (CRISM) on board Mars Reconnaissance Orbiter (MRO) detected distinct units with elevated spectral signatures of either hematite, phyllosilicates, or sulfates along the lower slopes of Mt. Sharp (Fraeman et al., 2016). These sedimentary strata record major paleoclimatic changes and have the potential for preserving evidence of ancient habitability. The rover explored the phyllosilicate-bearing region of lower Mt. Sharp from Sol (Martian day) 2300 to Sol 3072 of the mission, in what has been informally named the "Glen Torridon (GT) campaign" (Bennett et al., this issue).

Phyllosilicates indicate the presence of ancient near-neutral pH waters and, on Earth, are associated with enhanced preservation of organic molecules, so they have major implications for past Martian habitability (Keil & Mayer, 2013; Summons et al., 2011). The GT region underlies a sulfate-bearing unit and therefore records a period of Martian geological history prior to a major environmental shift (Grotzinger & Milliken, 2012). Exploration of the region can provide a

This article is protected by copyright. All rights reserved.

Accepted Article

framework to understand the environmental changes that allowed for the formation of the sulfate-bearing strata (Bennett et al., this issue; Fox et al., 2020).

Figure 1. Stratigraphic column showing drill samples acquired during the GT campaign (and two samples from Vera Rubin ridge that are discussed in this manuscript, HF and RH). See Figure S1 for a complete stratigraphic column from the MSL mission through the GT campaign. Column credit: MSL Sed-Strat Working Group.

Glen Torridon is a trough to the southeast of the Vera Rubin ridge (VRR) that overlaps substantially with the orbital spectral signatures of phyllosilicates. The region has been divided into several lithological units. The lowest portions of the GT trough consist of a continuation of hundreds of meters of mudstones known as the Murray formation. This portion of the GT is part of the Jura member, which is stratigraphically equivalent to the Jura member on VRR. Stratigraphically above the Murray formation was an observed change in lithology that warranted the naming of a new unit, the Carolyn Shoemaker formation, which was subdivided into the Knockfarril Hill member (KHm), and the Glasgow member (Gm) (Bennett et al., this issue) (Figure 1). *Curiosity* also completed a 'mini-campaign' by investigating and ascending the overlying Greenheugh pediment. The mini-campaign determined that the unconformable pediment capping unit was part of the Stimson formation of the Siccar Point group, which was encountered earlier in the mission (Banham et al., this issue). Eight drilled samples from the GT campaign are discussed in this work: Kilmarie (KM) from the Jura member, Glen Etive 1 and 2 (GE1 and GE2), Mary Anning (MA), and Groken (GR) from the KHm, Glasgow (GG) and Hutton (HU) from Gm, and Edinburgh (EB) from the Greenheugh pediment capping unit (Figure 2).

Geochemical analyses indicated that the GT region is compositionally similar to Murray formation rocks encountered earlier in the mission but with elevated abundances of crystalline phyllosilicates and minor changes in volatile chemistry indicative of a complex geologic history. Data from the Alpha Particle X-ray Spectrometer (APXS) showed that the GT region is

This article is protected by copyright. All rights reserved.

Accepted Article

geochemically similar to median Murray formation composition (O'Connell-Cooper et al., this issue; Berger et al., 2020). The Chemistry and Mineralogy (CheMin) X-ray Diffractometer (XRD) detected elevated abundances of phyllosilicates in the GT region, consistent with the orbital data, and lower amounts of hematite compared to the Vera Rubin ridge (Thorpe et al., this issue). The Sample Analysis at Mars (SAM) instrument suite detected evolved gases consistent with the presence of Fe-sulfates/sulfides (e.g., $FeSO_4$, FeS_2), Mg-sulfates (e.g., $MgSO_4$), and chlorides (e.g., NaCl, $CaCl_2$), with the notable absence of abundant nitrates (NO_3^-) and oxychlorines (e.g., perchlorates/chlorates, ClO_4^-/ClO_3^- salts) (McAdam et al., this issue.; McAdam et al., 2021). The SAM gas chromatography-mass spectrometry (GCMS) and wet chemistry experiments identified various organic molecules including nitrogen-, oxygen-, and chlorine-containing molecules as well as polycyclic aromatic hydrocarbons. SAM GCMS also revealed the highest diversity and abundance of sulfur-bearing aliphatic and aromatic organic compounds yet detected in Gale crater (Millan et al., this issue.).

Figure 2. Mars Hand Lens Imager (MAHLI) images of the drill holes acquired during the GT and Greenheugh pediment campaigns. Drill holes are ordered according to stratigraphy but do not reflect true vertical distances between samples. Glen Etive 1 and 2 were drilled from the same rock for two sets of experiments. Each drill hole is ~1.6 cm in diameter. Courtesy of NASA/JPL-Caltech/MSSS.

1.2 Sulfur on Mars and its Astrobiological Relevance

The sulfur cycle is a complex geochemical cycle with great relevance and impact on terrestrial ecosystems (Rogan et al., 2005) and with important astrobiological implications. Sulfur is an essential element for terrestrial organisms' life cycles (Clark, 1998). These cycles consist of the transformation of reduced sulfur to its oxidized forms, and vice versa, that go from the -2 oxidation state (reduced) to the +6 oxidation state (oxidized). This chemical modification supports life in Earth ecosystems, whereby organisms gain chemical energy with the transformation of

This article is protected by copyright. All rights reserved.

Accepted Article

sulfur from one oxidation state to another. Both sulfur oxidation and reduction reactions are the energy sources for metabolism by various microorganisms on Earth. The oxidation reactions from its reduced state can occur in both aerobic (i.e., with the presence of oxygen) and anaerobic (i.e., absence of oxygen) environments (Bosch et al., 2012; Percak- Dennett et al., 2017). In the latter case, these oxidation reactions are often mediated by phototrophic microorganisms (Bryant & Frigaard, 2006). In the case of aerobic or microaerophilic oxidation reactions, they require the presence of a neutral pH in the aqueous solution, which would be compatible with the presence of phyllosilicates in the GT region and with the measured pH of Martian soil (Quinn et al., 2011). The oxidation of reduced forms of sulfur towards the oxidized ones mediates the production of H^+, promoting acidification of the environment.

The reduction of oxidized sulfur phases energetically supports sulfate-reducing microorganisms as well. This second part of the cycle is complementary to the first and allows these organisms to gain energy from the reduction reactions. Sulfide-oxidizing organisms could take advantage of the availability of a variety of oxidants on contemporaneous Mars (Lasne et al., 2016).

Forms of reduced sulfur are also invoked at one point or another in the majority of the various hypotheses of the abiotic chemistries for the origin of life (B. Clark et al., 2021). Reduced sulfur compounds also play substantial roles in the intermediate metabolism of living organisms on Earth.

Sulfur has been detected over much of the Martian surface by orbital and *in-situ* measurements (King & McLennan, 2010). The majority of sulfur detected *in-situ* at Gale crater has been oxidized in the form of sulfate. Ca-sulfate was detected in Gale crater surface materials in the form of white veins by the rover's Chemistry and Camera (ChemCam) instrument (Gasda

This article is protected by copyright. All rights reserved.

Accepted Article

et al., 2020; Kronyak et al., 2019). Various crystalline sulfates (i.e., gypsum, bassanite, anhydrite, and jarosite) have been detected in drill samples by CheMin, with Ca-sulfates occasionally reaching over 20 wt% of the crystalline fraction (Rampe et al., 2020; Thorpe et al., this issue; Vaniman et al., 2018). Other sulfates, such as Mg-sulfates and Fe-sulfates have been inferred from data collected by the SAM instrument suites's evolved gas analysis (EGA) mode (e.g., Sutter et al. 2017; Stern et al. 2018; McAdam et al. 2020), which records the volatile decomposition products released by compounds in solid samples during heating. While crystalline Ca-sulfates have been detected by CheMin, their decomposition temperature is above the SAM oven temperature range, which prevents their detection by SAM EGA on Mars. SAM-EGA can be especially useful for identifying compounds that are either X-ray amorphous or below the CheMin minimum detection limit (~1-2 wt.%).

While oxidized sulfur is ubiquitous on Mars today, sulfides remain an important part of Martian geologic history. Igneous sulfides, in addition to sulfates, have frequently been observed in Martian meteorites (up to ~2300 ppm sulfide), and analysis of meteorite sulfur has indicated the common assimilation of sulfur into magmas over much of Martian history (Franz et al., 2014 and references therein). At Gale, the first apparent detection of sulfide was in the John Klein (JK) and Cumberland (CB) drilled samples, which were collected early in the mission in the Sheepbed member of the Yellowknife Bay formation (Vaniman et al., 2014). CheMin reported pyrrhotite and/or pyrite in both JK and CB, though the mineral abundances were near the instrument's detection limit (Vaniman et al., 2014), and subsequent reinterpretations of the XRD data have not reported crystalline sulfide detections (Morrison et al., 2018). However, SAM analyses of these samples support the presence of trace and/or amorphous sulfide based on sulfur isotope analysis and quadratic discriminant analysis comparing the SAM data to SAM-like laboratory analogue

This article is protected by copyright. All rights reserved.

Accepted Article

analyses (Franz et al., 2017; Wong et al., 2020). EGA of other samples, such as the Rocknest Martian fines, suggested the presence of sulfide based on the detection of evolved gases, such as H_2S (Leshin et al., 2013; McAdam et al., 2014; Ming et al., 2014; Sutter et al., 2017). However, the evolution of H_2S may also occur due to oven reactions between oxidized sulfur (SO_2) and H_2 ($SO_2 + 3H_2 \rightarrow H_2S + 2H_2O$) (McAdam et al., 2014). H_2 evolved during EGA may have several sources, including water fragmentation, organic molecules, or instrument effects, though its exact nature is under investigation (McAdam et al., this issue and references therein). SAM has also detected the thermal decomposition products of various sulfur-containing organic compounds, such as thiophenes, at high temperatures (Eigenbrode et al., 2018; Millan et al., this issue). Overall, SAM analyses of surface materials suggest the presence of reduced sulfur in various locations throughout the rover's traverse.

1.3 Approach of this Work

This article presents the results of three methods of analyzing EGA data to detect whether Glen Torridon samples contain sulfide, particularly at trace levels below the detection limits of CheMin. The peak temperatures of SO_2 evolutions were used to identify sulfur and associated metals (i.e., Mg sulfate vs. Fe sulfate/sulfide) in a sample. Additionally, multivariate statistical comparisons of SAM EGA data and SAM-like laboratory analogue data were used to identify Gale crater samples that were likely to contain sulfide. Finally, sulfur isotope values were calculated from SAM-evolved SO_2 to potentially identify which SO_2 peaks are likely derived from the oxidation of a sulfide versus decomposition of a sulfate. These combined analyses represent a novel approach to identifying sulfide in Martian samples from EGA data that is more powerful than any single method, providing greater confidence for any detection. We also discuss

This article is protected by copyright. All rights reserved.

Accepted Article

implications for habitability and geologic history of the Glen Torridon region in Gale crater based on the detection of sulfide.

2 Materials and Methods for Evolved Gas Analysis

2.1 Sample Analysis at Mars Evolved Gas Analysis (SAM EGA)

The SAM instrument suite was designed to investigate the volatile organic and inorganic chemistry of Martian samples. SAM EGA experiments study the gases released from solid samples during a ramped heating process. The SAM EGA procedure has been detailed previously (e.g., Mahaffy et al. 2012; Sutter et al. 2017; McAdam et al. 2020). In short, solid samples from the drill or scoop are delivered to quartz sample cups, which are then sealed in one of the two SAM pyrolysis ovens. Under a constant He flow of 0.8 sccm at 25 mbar, samples are heated to ~850˚C with a temperature ramp rate of 35˚C/min. Evolved gases are moved by the He carrier gas directly to the quadrupole mass spectrometer (QMS) for analysis. The QMS records the ionized volatiles as a mass-to-charge (*m/z*) ratio with a scan from *m/z* 2 to *m/z* 535. The data are then visualized in plots showing intensity versus temperature for any given *m/z* (Franz et al., 2020).

2.2 Laboratory Samples and Preparation

A variety of sulfur compounds and mixtures of sulfur compounds with Mars-analogue phases were analyzed on a SAM-like EGA system at Goddard Space Flight Center (GSFC) for use in the quadratic discriminant analysis. These analogue samples included oxidized (melanterite, ferric sulfate hydrate, jarosite, and kieserite) and reduced (pyrite and troilite/pyrrhotite) sulfur along with mixtures of various chlorine-, water-, or carbon-bearing phases (Table S1). These compounds were chosen to investigate specific volatile evolutions and interactions within simple mixtures relevant to SAM observations. A range of Fe-bearing sulfates (melanterite, ferric sulfate hydrate, and jarosite) were chosen because Fe-sulfates have been identified on Mars as both

This article is protected by copyright. All rights reserved.

Accepted Article

crystalline (jarosite; e.g., Morrison et al., 2018; Rampe et al., 2020) and amorphous phases (Smith et al., accepted; Sutter et al., 2017). Observations of these Fe-sulfates are consistent with predictions from models involving hydration, pH, and oxidation (King & McSween Jr., 2005). Jarosite purity was confirmed by X-ray diffraction (Wong et al., 2020). While the hydration state of Fe-sulfates can change over time (Hyde et al., 2011), the effects on SO_2 evolution temperature are minimal (McAdam et al., 2014). Kieserite ($MgSO_4 \cdot H_2O$) was chosen because hydrated Mg-sulfates are expected to be abundant on Mars from orbital observations (Milliken et al., 2010) and Mg-sulfates have been interpreted from SAM data (McAdam et al., this issue; Sutter et al., 2017). Ca-sulfates, despite their observation by CheMin (Rampe et al., 2020), were not included in this study because of their high decomposition temperatures that are above the SAM oven range (Lewis et al., 2015; Sutter et al., 2017). Likewise, Na- and K-sulfates also decompose at temperatures above the SAM range and were not included (King et al., 2018; Lewis et al., 2015). While thermogravimetric analyses indicate that hydrated Ca-, Na-, and K-sulfates undergo mass loss during heating, the loss is due primarily to dehydration rather than SO_2 evolution (Balić-Žunić et al., 2016; King et al., 2018; Kloprogge et al., 2004). The sulfides were chosen based on their detection by CheMin (Vaniman et al., 2014) and interpretation of SAM data (Franz et al., 2017). Laboratory sulfide purity was determined by X-ray diffraction (Wong et al., 2020). Chlorine phases were chosen due to the observations of chlorides and (per)chlorates on Mars (J. Clark et al., 2021; Glavin et al., 2013). The phyllosilicate nontronite was chosen because evidence of similar phyllosilicates has been observed in several samples (e.g., Bristow et al., 2015, 2018; McAdam et al., this issue ; Thorpe et al.,this issue). The carbon-bearing species were chosen to represent various oxidation states of carbon that could potentially be found on Mars and affect

This article is protected by copyright. All rights reserved.

Accepted Article

EGA results, including contamination within SAM (Eigenbrode et al., 2018; Freissinet et al., 2019; Glavin et al., 2013; Lewis et al., 2021).

While the laboratory-analyzed compounds were typically crystalline, it is important to note that Martian samples are a mix of crystalline and amorphous phases. On Mars, only jarosite and Ca-sulfates (anhydrite, bassanite, and gypsum) have been repeatedly observed by CheMin (with possible observations of pyrite and pyrrhotite at John Klein and Cumberland near the detection limit of ~1wt. % for crystalline phases) (Rampe et al., 2020; Vaniman et al., 2014). Importantly, CheMin analyses reveal large proportions of amorphous materials (Achilles et al., 2020; Rampe et al., 2020). Other MSL instrumentation, such as SAM, APXS, and ChemCam have been used in conjunction with CheMin to constrain the composition of the X-ray amorphous materials (Cousin et al., 2015; Dehouck et al., 2014; Smith et al., 2021; Sutter et al., 2017). It has been calculated that 20-90% of the total sulfur of a sample is in the amorphous component and the sulfur is primarily composed of Fe-, Mg-, and/or Ca-sulfates (Smith et al., accepted). Amorphous phases may have similar decomposition temperatures as their crystalline counterparts, as observed for ferric sulfate (McAdam et al., 2014). While other factors may impact observed decomposition temperatures (e.g., particle size, sample size, and mixtures (Archer et al., 2013; Lewis et al., 2021; McAdam et al., 2016)), the use of a large temperature range during analysis minimizes these effects (Section 3.1 and Wong et al., 2020).

All solid compounds were mixed with inert, amorphous fused silica (typically 9:1 fused silica:sulfur by mass) to act as a non-volatile-bearing matrix to simulate the bulk Martian sample (Conrad et al., 2012). Such mixtures, while not 1:1 comparisons to Mars samples, allow for the interpretation of Martian data from simpler, known analyses. Solid mixtures were either combined using a sterile, organic-free steel mixing tool or ground together by a solvent-washed mortar and

This article is protected by copyright. All rights reserved.

Accepted Article

pestle for three minutes. The mixtures were sieved to a size fraction <150 μm, comparable to powdered samples analyzed by SAM. The same set of samples (Table S1) was used for statistical comparisons to Mars samples through the Vera Rubin ridge and has been described in detail by Wong et al. (2020).

2.3 Laboratory Evolved Gas Analysis

The laboratory EGA instruments used in this work were designed to have similar operating conditions to the SAM oven and QMS so that resulting evolved gas data could be directly compared to SAM EGA data. The EGA work used for the quadratic discriminant analysis comparisons was conducted at GFSC with an Agilent 5975T Low Thermal Mass Gas Chromatograph/Mass Selective Detector (LTM GC/MSD) attached to a Frontier PY-3030D pyrolysis oven (Wong et al., 2020). Samples were first held at 75˚C for up to 31 minutes under a constant He flow rate of 35˚C/min (50 mL/min at 30 mbar) to allow for the desorption of adsorbed volatiles (e.g., atmospheric water) on the sample without thermal decomposition. Samples were heated in inert stainless steel pyrolysis cups in the oven to at least 850˚C with the same flow conditions. The He flow was routed to the quadrupole mass spectrometer for analysis of evolved volatiles with *m/z* values ranging up to 200.

3 Data and Analyses

3.1 Quadratic Discriminant Analysis

Known samples (Table S1) were analyzed using a laboratory SAM-like EGA system (Section 2.3) and then statistically compared to SAM EGA data using quadratic discriminant analysis (QDA). QDA is a supervised multivariate machine learning statistical method that is used to classify unknown items with a set of variables into classes based on a known training dataset. During QDA, a model is built from a training dataset (laboratory EGA volatiles from sulfides and

This article is protected by copyright. All rights reserved.

Accepted Article

sulfates). Using this training dataset, an unknown sample with the same variables (SAM EGA sample) is put into one of two classes (sulfide or no sulfide) based on its maximum probability of being in a class given the values of its variables. This method is commonly used to classify unknowns samples into distinct categories and has been used previously on Mars for identifying Martian samples that likely contained reduced sulfur (Wong et al., 2020). In addition to the classification, the posterior probability was calculated for each sample's classification. The reported posterior probability (as a percent value) for a given sample indicates the probability that the Martian sample correctly classifies with the laboratory sulfide. A sample is considered likely to contain sulfide when the posterior probability is >50%. All QDA work was performed in Python 2.7.14 as described previously (Wong et al., 2020).

Recorded counts of evolved *m/z* ratios corresponding to the evolved volatiles SO_2, COS, CS_2, CO_2, and 1,3-bis(1,1-dimethylethyl)-1,1,3,3-tetramethyldisiloxane (i.e., bi-silylated water (BSW)) from 75˚C-600˚C were used for the QDA variables dataset. These volatiles were chosen because they can help discriminate between sulfates and sulfides. In laboratory experiments, COS and CS_2 were shown to evolve significantly more (typically 1-3 orders of magnitude) from sulfides than from sulfates (Wong et al., 2020). CO_2 was considered a potential source of carbon for COS and CS_2 production from sulfide, and it could have been derived from background, carbonate decomposition, organic decarboxylation, or organic oxidation by O_2 (Francois et al., 2016; Lewis et al., 2021; Lewis et al., 2015; Sutter et al., 2017). SO_2 evolved during sulfate decomposition or sulfide oxidation (e.g., by O_2, H_2O, or CO_2; Table S2) could also be a sulfur source for COS and CS_2 (e.g, $SO_2 + 3CO \rightarrow COS + 2CO_2$; Table S2). BSW is the product of N-tert-butydimethylsilyl-N-methyltrifluoroacetamide (MTBSTFA) hydrolysis (Table S2) that occurs in all SAM EGA experiments (Eigenbrode et al. 2018, supporting information). MTBSTFA is one of two chemical

This article is protected by copyright. All rights reserved.

Accepted Article

derivatization reagents used for SAM wet chemistry experiments. MTBSTFA is present in the Sample Manipulation System (SMS) due to a leak in at least one of the sample cups containing it and from carry-over after the wet chemistry experiments (Glavin et al., 2013). The amount of MTBSTFA varies depending on sample size (due to surface area available to adsorb) and length of time allowed for adsorption. BSW was used as a tracer for MTBSTFA contamination that can result in interfering *m/z* ratios or oven reactions that would otherwise cause false positive sulfide detections. The volatiles described above can form during EGA from a variety of reactions, some of which are shown in Table S2. All counts were normalized by total sample size and then log transformed for comparisons.

3.2 Sulfur Isotope Calculations

Sulfur isotopes (reported as $\delta^{34}S$ Vienna-Canyon Diablo Troilite, V-CDT) were calculated from SAM-evolved peaks of $^{32}SO_2$ (*m/z* 64) and $^{34}SO_2$ (*m/z* 66) without *a priori* knowledge of source material. Evolved counts were "dead time" corrected to account for the time between events to be counted as separate and for high count rates (Franz et al., 2014). Counts were subsequently background corrected by subtracting average counts prior to the start of heating. Ratios of $^{34}SO_2/^{32}SO_2$ were calculated for each simultaneously collected *m/z* 66 and *m/z* 64 during the evolution of an SO_2 peak. The average ratio of $^{34}SO_2/^{32}SO_2$ was calculated for the values under the peak when the ratio appeared stable and the associated error with this average was carried through calculations. The $^{34}SO_2/^{32}SO_2$ was then corrected for interfering isotopologues (i.e., $^{32}S^{16}O^{18}O$, $^{33}S^{17}O^{16}O$, and $^{32}S^{17}O^{17}O$) that would artificially increase the apparent ratio. This subtraction effectively yielded a ratio of $^{34}S/^{32}S$, which was compared to the V-CDT standard ratio to calculate a delta value according to the formula:

$$\delta^{34}S = 1000 \times [(^{34}R_{sample}/^{34}R_{V\text{-}CDT}) - 1],$$

This article is protected by copyright. All rights reserved.

Accepted Article

where $^{34}R_{sample} = {}^{34}S/{}^{32}S = m66/m64 - 2x^{18}R - 2x^{17}Rx^{33}R - {}^{17}R^2$

and $^{18}R = {}^{18}O/{}^{16}O$, $^{17}R = {}^{17}O/{}^{16}O$, and $^{33}R = {}^{33}S/{}^{32}S$

accounting for the isotopologue contributions mentioned above. In this work the following assumptions about the oxygen and sulfur isotope ratios were made:

(1) An assumed $\delta^{18}O$ of +50‰ (based on the modern Martian atmosphere) was used to calculate ^{18}R (Webster et al., 2013),

(2) ^{17}R was calculated from Martian meteorites $\Delta^{17}O$=+0.32‰ where $\Delta^{17}O=\delta^{17}O-0.52x\delta^{18}O$ (Franchi et al., 1999),

(3) ^{33}R was assumed to be equal to the V-CDT standard (Franz et al., 2017).

These sulfur isotope calculations follow the extended methods described by Franz et al. (2017) and were only calculated for SAM data. A range of $\delta^{34}S$ values from -47±14‰ to 28±7‰ was previously reported for Gale crater samples by Franz et al. (2017). A model involving atmospheric processing of volcanic sulfur gases and equilibrium fractionation between sulfide and sulfate in a hydrothermal groundwater system was described to explain the wide $\delta^{34}S$ range. Photolysis and oxidation of sulfur gases in the atmosphere can result in isotopically-enriched products with relatively small depletions in the source pools. Equilibration in a hydrothermal system can fractionate the isotopes, with ^{34}S being preferentially incorporated into sulfates/sulfites, leading to the isotopic depletion of resultant sulfides. Based on this model, here, enriched values $\delta^{34}S$ are considered to represent sulfates, while highly depleted values represent sulfides, and $\delta^{34}S$ near 0 may be from mantle-derived sulfide or sulfate.

A schematic summary of the methods used in these analyses can be found in Figure S2.

This article is protected by copyright. All rights reserved.

Accepted Article

4 Results and Discussion

4.1 Sulfur EGA Results

A summary of the results for the 13 (sub-)samples analyzed by SAM EGA is provided in Table 1. Refer to Figures S3 and S4a-g for additional details on QDA clustering and QDA volatiles, respectively. EB has consistent evidence for the presence of a sulfide from the three methods of analysis. KM also appears likely to contain reduced sulfur.

Table 1. Summary of sulfur EGA, QDA, and S isotope results for all drilled samples in the GT campaign and Greenheugh pediment mini-campaign. Sample abbreviations are listed in the first column. The peak temperature of evolved SO_2 for the release in the interpreted Fe-sulfate/sulfide region is given in the second column. "Low temperature" (<400˚C) SO_2 releases have their peaks listed in the third column, if applicable. The fourth column lists the posterior probability of a sample containing sulfide based on QDA. The final column lists the $\delta^{34}S$ values calculated for the main SO_2 release in the Fe sulfate/sulfide region.

Figure 3. Evolved SO_2 from samples analyzed by the SAM instrument suite during the GT campaign and the pediment capping unit mini-campaign. SO_2 data were normalized to the maximum intensity of evolved SO_2 during EGA to focus on differences in temperatures. Different colors represent different EGA runs of the same sample (black=first, red=second, green=third). KM=Kilmarie, GE=Glen Etive, MA=Mary Anning, GR=Groken, GG=Glasgow, HU=Hutton, EB=Edinburgh

Figure 4. Low temperature evolution of SO_2 from 50˚C - 400˚C. Vertical axes have been adjusted to show the lower intensity SO_2 releases in this temperature range compared to Figure 3. EB is the only sample with a clear low-temperature SO_2 peak. Black=1st sample, red=2nd sample, green=3rd sample. KM=Kilmarie, GE=Glen Etive, MA=Mary Anning, GR=Groken, GG=Glasgow, HU=Hutton, EB=Edinburgh

Kilmarie (KM, drilled on Sol 2384) was the first sample analyzed by SAM during the GT campaign and was acquired from the GT Jura member of the Murray formation. Two previous samples of the Jura (Highfield and Rock Hall) were studied by SAM at Vera Rubin ridge, both of which likely contained reduced sulfur based on QDA (Wong et al. 2020). Two subsamples of KM (KM1 and KM2) were analyzed by SAM EGA and showed similar SO_2 evolution profiles (Figure 3). Both KM samples evolved SO_2 peaks consistent with Fe-sulfate/sulfide (~560˚C) and Mg-sulfate (~770˚C). Based on QDA, the posterior probabilities of KM1 and KM2 clustering with the

This article is protected by copyright. All rights reserved.

Accepted Article

laboratory sulfides were 97% and 63%, respectively (Table 1, Figures S3 and S4a). These posterior probabilities are consistent with the VRR Jura samples and Sheepbed mudstone samples. The $\delta^{34}S$ value of KM1 was most consistent with sulfur derived from a sulfide, with $\delta^{34}S = -21 \pm 19‰$, while KM2 was effectively unconstrained, with $\delta^{34}S = 0 \pm 20‰$ (Table 1).

Several drill samples of the KHm from the Carolyn Shoemaker formation were obtained during the GT campaign. Two adjacent Glen Etive (GE) samples from the same rock target were drilled (Sols 2486 and 2527) after KM. GE1 and GE2 represent EGA results from the first drill hole while GE3 is from the second drill hole. Mary Anning (MA), drilled on Sol 2838, was also a sample of the KHm. MA was chosen as a drill target to conduct a search for organic molecules in the KHm at a site that was stratigraphically similar to earlier GE samples. Groken (GR) was investigated due to its elevated Mn detections and was drilled next to MA on Sol 2910. A total of six EGA experiments were performed on these samples (three subsamples of GE, two of MA, and one of GR). Despite the samples all coming from the KHm, their SO_2 profiles were distinct (Figure 3). All of the analyses showed SO_2 releases consistent with Fe-sulfide/sulfate, though the GR Fe-sulfate/sulfide SO_2 peak evolved at a slightly lower temperature than the GE1, GE3, or MA1 samples. GE1 and GE2 also had high-temperature SO_2 releases consistent with Mg-sulfate. GR and GE1 had SO_2 peaks near 720˚C, consistent with an Fe- or Mg-sulfate. Both MA samples, on the other hand, had generally narrower peaks consistent with Fe-sulfide/sulfate and no Mg-sulfate. The QDA results were not consistent with laboratory sulfides in any of the KHm samples analyzed by SAM. For QDA, the highest posterior probability was 11% for GE2, which is less than the 50% cutoff for being considered likely to contain reduced S (Table 1, Figures S3 and S4b-d). The KHm samples did show a range of $\delta^{34}S$ values from $-14 \pm 5‰$ (GE3) to $20 \pm 4‰$ (GE1) (Table 1). While

This article is protected by copyright. All rights reserved.

Accepted Article

GE3 did have a moderately depleted $\delta^{34}S$, other evidence was not fully consistent with a sulfide. Overall, the analyses of the KHm samples were consistent with the presence of sulfates only.

Glasgow (GG), drilled on Sol 2754, was a sample from the Glasgow member of the Carolyn Shoemaker formation. Two subsamples of GG were analyzed by EGA. Both GG1 and GG2 had SO_2 evolutions consistent with Fe-sulfate/sulfide, while only GG2 had a peak consistent with Mg-sulfate (Figure 3). QDA results suggested that neither sample was consistent with the laboratory sulfides (Table 1, Figures S3 and S4e). The calculated $\delta^{34}S$ values from the Fe-sulfide/sulfate peak were highly enriched at 5 ± 9‰ and -5 ± 9‰ for GG1 and GG2, respectively (Table 1). These isotope values were consistent with a sulfate or a sulfide. While isotope and temperature analyses are ambiguous, the QDA results suggested that the GG samples were not likely to contain sulfide.

The Greenheugh pediment mini-campaign was conducted to investigate rocks that may provide insight into diagenetic fluids that altered the Glen Torridon rocks. Two samples were associated with this pediment mini-campaign: Hutton (HU, drilled Sol 2668) and Edinburgh (EB, drilled Sol 2711). Two SAM analyses were performed on the HU drill sample, which was chosen as a drill target due to its proximity to the basal unconformity. HU was a sample from the Glasgow member and was hypothesized to have been influenced by ancient fluid runoff from the pediment. Only a single SAM analysis was conducted on EB, which was taken from the Greenheugh pediment capping unit. Both HU samples generally resembled the GG and MA SO_2 evolutions, with only Fe-sulfate/sulfide peaks observed (Figure 3). HU was not consistent with laboratory sulfide according to QDA (Table 1, Figures S3 and S4f). The $\delta^{34}S$ values of HU1 and HU2 were enriched at 18 ± 6‰ and 21 ± 4‰ (Table 1), suggestive of a sulfate formed from equilibrium fractionation. While HU sulfur results were largely consistent with other GT samples, EB had

This article is protected by copyright. All rights reserved.

Accepted Article

entirely different results. The primary SO_2 peak evolution of EB was again consistent with Fe-sulfate/sulfide (Figure 3). However, there was also a significant peak of SO_2 at ~300˚C, which may be consistent with a sulfur source such as sulfonic acids, elemental sulfur, or the oxidation of a sulfide (Franz et al., 2017; McAdam et al., 2020). Such a low temperature peak was not observed in any of the other GT samples (Figure 4). The shape of the EB SO_2 EGA profile was comparable to laboratory-run FeS (Figure S5). Furthermore, the quadratic discriminant analysis clustered EB with the laboratory sulfides (Table 1, Figures S3 and S4g), suggesting the presence of a sulfide reacting with carbon gases (Table S2). As an independent, third line of evidence, the $\delta^{34}S$ calculated from SO_2 evolved during SAM-EGA was depleted at -27±7‰, consistent with a sulfide formed during equilibrium fractionation or hydrothermal alteration (Table 1). The ~300˚C peak of SO_2 observed in EB was too small to calculate a $\delta^{34}S$ value.

4.2 Discussion

4.2.1 Sulfides in Samples from the GT Campaign

Most of the samples analyzed by SAM during the GT campaign produced results consistent with the presence of sulfates rather than sulfides. The widespread occurrence of sulfates in the GT region is plausible given the ubiquity of sulfates on Mars and the oxidizing conditions near the surface. However, two of the GT samples (KM and EB) had multiple lines of evidence for the presence of reduced sulfur. These two samples had EGA, QDA, and S isotope evidence that were generally consistent with a sulfide. KM1, KM2, and EB are shown as a distinct group in QDA-variable space in Figure S2.

The evolution temperature of the largest release of SO_2 during KM EGA was consistent with either a sulfide or sulfate, but the QDA clustering and depleted $\delta^{34}S$ values in the KM sample from the Jura member strongly suggested the presence of a sulfide. The presence of a sulfide in

This article is protected by copyright. All rights reserved.

Accepted Article

KM was also consistent with previously reported results from the Vera Rubin ridge where two Jura member samples, HF and RH, also clustered with laboratory sulfides in QDA (Wong et al., 2020). In Wong et al. (2020), it was hypothesized that the reduced sulfur on VRR was the result of mildly reducing, sulfite-containing diagenetic fluids in which the sulfite decomposed in disproportionation reactions to form reduced S. Such disproportionation reactions could occur quickly at elevated groundwater temperatures of ~150ºC (Kusakabe et al., 2000). Hydrothermal isotopic equilibration could additionally result in a depletion of $\delta^{34}S$ in sulfides (H B Franz et al., 2017). Given that KM was also a sample from the Jura member, it is possible that its reduced sulfur was from the same source. This would suggest that the lower strata of Glen Torridon were affected by at least some of the same diagenetic fluids as the upper strata of the VRR. Additionally, CheMin and SAM have reported detections of siderite ($FeCO_3$) in the KM sample at >2 wt. % abundance (Archer Jr. et al. 2020; Thorpe et al. this issue), suggesting the presence of reducing aqueous conditions during formation.

The EB sample had the strongest evidence for the presence of reduced sulfur based on the EGA profile of SO_2, the results of QDA, and the calculated $\delta^{34}S$. The shape of the SO_2 evolution in EB was consistent with laboratory-run troilite and pyrrhotite samples, though the temperatures of the peaks were ~100˚C higher in the SAM analysis (Figure S5). EB had a distinct SO_2 peak around 300˚C, which was potentially consistent with the oxidation of a sulfide. Small low-temperature SO_2 peaks have been observed in numerous samples on Mars, including CB, HF, and RH, all of which have similarly been identified as likely containing reduced sulfur (Wong et al. 2020). QDA and S isotopic compositions also agreed that a sulfide was likely present in the EB sample. EB represents the pediment capping unit, which is a sandstone from the Stimson formation. This overlying lithological unit was deposited unconformably on the Mt. Sharp group

This article is protected by copyright. All rights reserved.

Accepted Article

rocks, which have made up the majority of samples analyzed by the mission so far. The sulfide present within the capping unit may have been derived from sulfide/sulfate equilibration at elevated temperature or, perhaps, from the disproportionation of sulfite in groundwater to allow for the preservation of the depleted ^{34}S signal. While sulfide and sulfate (e.g., pyrite and gypsum) can coexist under the right Eh/pH conditions (King & McSween Jr., 2005), their isotopic equilibrium fractionation is kinetically inhibited at low temperatures and would be unlikely to account for the strongly depleted ^{34}S signal (Eldridge et al., 2016; Franz et al., 2017). Rocks that are stratigraphically equivalent to the Greenheugh pediment, where EB was collected, will be encountered again later in the mission as the rover continues up Mt. Sharp, which will allow for additional analyses of similar rocks. If reduced sulfur is widespread in these more recent strata, it could have provided an energy source for potential ancient microbes.

4.2.2 Potential Habitability in the GT Region

The detection of both oxidized and reduced sulfur in the Glen Torridon region samples could be indicative of a complete sulfur cycle in ancient times. The resulting materials with sulfur in a range of oxidation states could have provided potential energy sources to support a complex sulfur oxidation/reduction ecosystem.

In environments where there have been sedimentary deposits including lake bottom sludge, anoxic environments may be produced. When these types of environments are exposed to solar radiation on Earth, they can develop bacterial activity over time that, together with abiotic processes, give rise to the deposition of chemical gradients formed by different oxidation states of sulfur (among other elements) (Dang et al., 2019). The sulfur in variable oxidation states may be used as metabolic substrates by various microorganisms. The presence of sunlight promotes the development of photosynthetic ecosystems that oxidize the reduced forms of sulfur in the absence

This article is protected by copyright. All rights reserved.

Accepted Article

of oxygen, as is the case for green and purple sulfur bacteria (Bryant & Frigaard, 2006). Other chemolithotrophic microbes, such as *Acidithiobacillus* and *Beggiatoa* species, can also be supported by oxidative chemical reactions using different inorganic electron donors such as hydrogen sulfide (H_2S), elemental sulfur (S^0), sulfite (SO_3^{2-}), and thiosulfate ($S_2O_3^{2-}$) (Ghosh & Dam, 2009). The resulting oxidized sulfur (as sulfate) can, in turn, be a metabolic substrate for sulfate reducers, such as *Desulfovibrio* and *Archaeoglobus* species, giving rise again to reduced sulfur (Muyzer & Stams, 2008). Therefore, the co-occurrence of oxidized and reduced sulfur supports the possibility of a past ecosystem sustained by sulfur redox reactions.

While the presence of multiple oxidations states of sulfur could have supported habitability for a hypothetical microbial ecosystem as described above, the sulfur could have had numerous sources. For example, minerals with oxidized and reduced sulfur can achieve chemical equilibrium at room temperature (King & McSween Jr., 2005). Multiple oxidations states of sulfur may also be the product of sulfur disproportionation (Kusakabe et al., 2000; Matsuzaki et al., 1978; Pryor, 1960; Wong et al., 2020). Alternatively, it is possible that the sulfur was delivered from a sulfide-containing basaltic source that underwent minimal or partial alteration (McAdam et al., 2014). The observation of mixed sulfur oxidation states could also be due to multiple sources of sulfur, such as sulfates (crystalline and/or amorphous) and preserved reduced sulfur in organic molecules (Eigenbrode et al., 2018; Millan et al., this issue). Regardless of source, the presence of both oxidized and reduced sulfur has interesting implications toward the habitability of the Glen Torridon region.

4.2.3 Complementary Sulfur Analyses

This work presents numerous avenues to aid in determining whether Martian samples contain reduced sulfur. Release of SO_2 during EGA is among the first possible indicators of sulfur

This article is protected by copyright. All rights reserved.

Accepted Article

oxidation state. While SO_2 is readily produced from the thermal decomposition of sulfates during EGA, it can also form during sulfide oxidation (Table S2). Based on laboratory data, SO_2 peaks around 500˚C-600˚C are generally consistent with either Fe-sulfate or Fe-sulfide decomposition. Furthermore, low temperature peaks near 300˚C may be consistent with a source such as a sulfide, elemental sulfur, or sulfonic acids. Taken together, there is not a unique solution from EGA temperature alone, especially given that multiple sulfur compounds from laboratory analyses may match the SO_2 release in a Martian sample.

Quadratic discriminant analysis adds another method of determining the oxidation state of sulfur using SAM EGA data and laboratory analogue data. From the laboratory analyses, it was clear that sulfides consistently evolved the reduced carbon-sulfur gases COS and CS_2, which were broadly interpreted as reaction products between the sulfide and CO/CO_2 (Table S2) in the system (Wong et al. 2020). These gases are key variables in the QDA and can be used to identify which Martian samples are likely to contain reduced sulfur. However, the amount and exact type of reduced sulfur cannot be reliably determined from this method, though QDA-determined sulfur is most likely an iron sulfide that is present at trace abundance and/or amorphous and therefore not detectable by CheMin. QDA also does not reveal information about the source of sulfur compounds inferred.

Sulfur isotopic compositions calculated from SAM EGA SO_2 data can provide valuable information about the oxidation state of sulfur. Possible sources of the sulfur can also sometimes be inferred from these values based on the observed fractionation. Highly depleted values are consistent with a sulfide formed during equilibrium fractionation between sulfide and sulfate over time. Depleted values may also be consistent with sulfide formed from the disproportionation of mid-valence sulfur compounds, such as sulfite. Values of $\delta^{34}S$ near zero suggest that the sulfur

This article is protected by copyright. All rights reserved.

Accepted Article

was derived from mantle material. This may be consistent with either igneous sulfides or sulfates formed from volcanic SO_2 rainout. More enriched sulfur isotopic values are consistent with sulfate formed during equilibrium fractionation, disproportionation reactions, or atmospheric processing.

Although S isotopic compositions from SO_2 evolutions can provide information on the oxidation state of sulfur, there are challenges associated with this method. The $\delta^{34}S$ values near zero can be ambiguous in that they could still represent either sulfide or sulfate. Additionally, some peaks are too small for accurate isotope values to be calculated due to the relatively low abundance of ^{34}S. The signal-to-noise ratio of an *m/z* 66 peak, from which ^{34}S is derived, can be too low for accurate calculation.

Each of our methods determining sulfur oxidation state from SAM EGA data complement each other well in different situations. SO_2 evolution peak temperatures can provide a quick insight into the presence of an iron-bearing sulfur compound. QDA can help distinguish whether that compound is a sulfide or sulfate. S isotopes can confirm the QDA finding if the $\delta^{34}S$ shows a strong enrichment or depletion. Alternatively, QDA can suggest whether an ambiguous $\delta^{34}S$ result (i.e., $\delta^{34}S$ near 0‰) corresponds to a sulfide. As the MSL mission continues to explore Gale crater for potential signs of habitability, it would be prudent to use all three types of analyses to identify sulfur oxidation states. These analyses further complement chemical and mineralogical work performed by the other instruments on the rover, such as APXS and CheMin to gain a more complete picture of Martian habitability.

5 Conclusions

The Glen Torridon campaign accomplished a long-held goal of the MSL mission: to explore the region of Gale crater with elevated orbital signatures for clay minerals and to assess its potential for ancient habitability. The work here specifically investigated the possible presence

This article is protected by copyright. All rights reserved.

Accepted Article

of reduced sulfur in the GT region and surrounding units using a combination of complementary methods analyzing SAM EGA data. Most of the samples did not have strong evidence for reduced sulfur except for Kilmarie and Edinburgh. Kilmarie may have been diagenetically altered by some of the same fluids as the Jura member on the nearby Vera Rubin ridge, resulting in reduced S. It is not yet clear why Edinburgh appears to contain reduced sulfur, though it presents an opportunity for further study as the rover is expected encounter the same strata later in the mission. The observation that most GT samples did not contain sulfide suggests that the GT region has been largely oxidized, consistent with most of the underlying samples at Gale crater. The presence of sulfides in two samples, however, suggests that reduced sulfur could have been available as an electron donor for putative chemolithotrophic metabolisms in a potentially habitable environment on ancient Mars.

Data Availability

All SAM raw data are available on the Planetary Data System at http://pds-geosciences.wustl.edu/missions/msl/ (Mahaffy, 2013). Laboratory data for the QDA comparisons are stored on the Harvard Dataverse (Wong, 2020). Laboratory EGA data used in Figure S5 and processed SAM data used for QDA are available on a separate Harvard Dataverse page (G. Wong, 2022).

Acknowledgments

We would like to thank the MSL Science and Engineering teams for the successful operation of the rover and its instruments making this work possible. We also thank the larger SAM team for their support in data collection and interpretation. We gratefully acknowledge NASA for support of the Mars Science Laboratory (*Curiosity* rover) mission and for support to the Mars Science Laboratory participating scientist program (C.H.H, J.L.E., A.C.M.). This work was supported by

This article is protected by copyright. All rights reserved.

Accepted Article

NASA Headquarters under the NASA Earth and Space Science Fellowship Program – Grant "80NSSC18K0205" (G.M.W.). G.M.W. also acknowledges the support from the Pennsylvania Space Grant Consortium. We thank Penny King for a thoughtful and thorough review as well as Editor Deanne Rogers and Associate Editor Mariek Schmidt for comments that have all greatly improved this manuscript.

References

Achilles, C. N., Rampe, E. B., Downs, R. T., Bristow, T. F., Ming, D. W., Morris, R. V, et al. (2020). Evidence for Multiple Diagenetic Episodes in Ancient Fluvial-Lacustrine Sedimentary Rocks in Gale Crater, Mars. *Journal of Geophysical Research: Planets*, *125*(8), e2019JE006295. https://doi.org/https://doi.org/10.1029/2019JE006295

Archer Jr., P. D., Rampe, E. B., Clark, J. V, Tu, V., Sutter, B., Vaniman, D., et al. (2020). Detection of Siderite (FeCO3) in Glen Torridon Samples by the Mars Science Laboratory Rover. *51st Lunar and Planetary Science Conference*, LPI Contrib. No. 2709.

Archer, P. D., Ming, D. W., & Sutter, B. (2013). The effects of instrument parameters and sample properties on thermal decomposition: interpreting thermal analysis data from Mars. *Planetary Science*, *2*(2), 1–21. https://doi.org/10.1186/2191-2521-2-2

Balić-Žunić, T., Birkedal, R., Katerinopoulou, A., & Comodi, P. (2016). Dehydration of blödite, Na2Mg(SO4)2(H2O)4, and leonite, K2Mg(SO4)2(H2O)4. *European Journal of Mineralogy*, *28*(1), 33–42. https://doi.org/10.1127/ejm/2015/0027-2487

Banham, S. G., Gupta, S., Rubin, D. M., Bedford, C. C., Edgar, L., Bryk, A., et al. (submitted). Evidence for seasonal- to millennial-scale wind fluctuations in an ancient aeolian dune field: Reconstruction of the Hesperian Stimson formation at the Greenheugh pediment, Gale crater, Mars. *Journal of Geophysical Research: Planets*.

Bennett, K., Fox, V., Bryk, A., Dietrich, W., Fedo, C., Dehouck, E., & Cousin, A. (submitted). An Overview of the Curiosity rover's Campaign in Glen Torridon, Gale Crater, Mars.

Berger, J. A., Gellert, R., Boyd, N. I., King, P. L., McCraig, M. A., O'Connell-Cooper, C. D., et al. (2020). Elemental Composition and Chemical Evolution of Geologic Materials in Gale Crater, Mars: APXS Results From Bradbury Landing to the Vera Rubin Ridge. *Journal of Geophysical Research: Planets*, *125*(12), e2020JE006536. https://doi.org/https://doi.org/10.1029/2020JE006536

Bosch, J., Lee, K.-Y., Jordan, G., Kim, K.-W., & Meckenstock, R. U. (2012). Anaerobic, Nitrate-Dependent Oxidation of Pyrite Nanoparticles by Thiobacillus denitrificans. *Environmental Science & Technology*, *46*(4), 2095–2101. https://doi.org/10.1021/es2022329

Bristow, T. F., Bish, D. L., Vaniman, D. T., Morris, R. V., Blake, D. F., Grotzinger, J. P., et al. (2015). The origin and implications of clay minerals from Yellowknife Bay, Gale crater, Mars. *American Mineralogist*, *100*(4), 824–836. https://doi.org/10.2138/am-2015-5077CCBYNCND

Bristow, T. F., Rampe, E. B., Achilles, C. N., Blake, D. F., Chipera, S. J., Craig, P., et al. (2018). Clay mineral diversity and abundance in sedimentary rocks of Gale crater, Mars. *Science*

This article is protected by copyright. All rights reserved.

Accepted Article

Advances, *4*(eaar3330). https://doi.org/10.1126/sciadv.aar3330
Bryant, D. A., & Frigaard, N. U. (2006). Prokaryotic photosynthesis and phototrophy illuminated. *Trends in Microbiology*, *14*(11), 488–496. https://doi.org/10.1016/j.tim.2006.09.001
Clark, B. C. (1998). Surviving the limits to life at the surface of Mars. *Journal of Geophysical Research*, *103*(E12), 28,545–28,555.
Clark, B. C., Kolb, V. M., Steele, A., House, C. H., Lanza, N. L., Gasda, P. J., et al. (2021). Origin of Life on Mars: Suitability and Opportunities. *Life*, *11*(6), 539.
Clark, J., Sutter, B., Archer, P. D., Ming, D., Rampe, E., McAdam, A., et al. (2021). A Review of Sample Analysis at Mars-Evolved Gas Analysis Laboratory Analog Work Supporting the Presence of Perchlorates and Chlorates in Gale Crater, Mars. *Minerals*. https://doi.org/10.3390/min11050475
Conrad, P. G., Eigenbrode, J. L., Heydt, M. O. Von Der, Mogensen, C. T., Canham, J., Harpold, D. N., et al. (2012). The Mars Science Laboratory Organic Check Material. *Space Science Reviews*, *170*, 479–501. https://doi.org/10.1007/s11214-012-9893-1
Cousin, A., Meslin, P. Y., Wiens, R. C., Rapin, W., Mangold, N., Fabre, C., et al. (2015). Compositions of coarse and fine particles in martian soils at gale: A window into the production of soils. *Icarus*, *249*, 22–42. https://doi.org/https://doi.org/10.1016/j.icarus.2014.04.052
Dang, H., Klotz, M. G., Lovell, C. R., & Sievert, S. M. (2019). Editorial: The Responses of Marine Microorganisms, Communities and Ecofunctions to Environmental Gradients . *Frontiers in Microbiology* . Retrieved from https://www.frontiersin.org/article/10.3389/fmicb.2019.00115
Dehouck, E., McLennan, S. M., Meslin, P.-Y., & Cousin, A. (2014). Constraints on abundance, composition, and nature of X-ray amorphous components of soils and rocks at Gale crater, Mars. *Journal of Geophysical Research: Planets*, *119*(12), 2640–2657. https://doi.org/https://doi.org/10.1002/2014JE004716
Eigenbrode, J. L., Summons, R. E., Steele, A., Freissinet, C., Millan, M., Navarro-González, R., et al. (2018). Organic matter preserved in 3-billion-year-old mudstones at Gale crater, Mars. *Science*, *360*(6393), 1096–1101.
Eldridge, D. L., Guo, W., & Farquhar, J. (2016). Theoretical estimates of equilibrium sulfur isotope effects in aqueous sulfur systems: Highlighting the role of isomers in the sulfite and sulfoxylate systems. *Geochimica et Cosmochimica Acta*, *195*, 171–200. https://doi.org/https://doi.org/10.1016/j.gca.2016.09.021
Fox, V. K., Bennett, K. A., Bryk, A., Arvidson, R., Bristow, T., Dehouck, E., et al. (2020). One Year in Glen Torridon: Key Results from the Mars Science Laboratory Curiosity Rover exploration of clay-bearing units. *51st Lunar and Planetary Science Conference*, LPI Contrib. No. 2833.
Fraeman, A. A., Ehlmann, B. L., Arvidson, R. E., Edwards, C. S., Grotzinger, J. P., Milliken, R. E., et al. (2016). The stratigraphy and evolution of lower Mount Sharp from spectral, morphological, and thermophysical orbital data sets. *Journal of Geophysical Research: Planets*, *121*(9), 1713–1736. https://doi.org/10.1002/2016JE005095
Franchi, I. A., Wright, I. P., Sexton, A. S., & Pillinger, C. T. (1999). The oxygen-isotopic composition of Earth and Mars. *Meteoritics & Planetary Science*, *34*(4), 657–661. https://doi.org/10.1111/j.1945-5100.1999.tb01371.x
Francois, P., Szopa, C., Buch, A., Coll, P., McAdam, A. C., Mahaffy, P. R., et al. (2016).

This article is protected by copyright. All rights reserved.

Magnesium sulfate as a key mineral for the detection of organic molecules on Mars using pyrolysis. *Journal of Geophysical Research: Planets*, *121*, 61–74. https://doi.org/10.1002/2015JE004884

Franz, H. B., Trainer, M. G., Wong, M. H., Manning, H. L. K., Stern, J. C., Mahaffy, P. R., et al. (2014). Analytical techniques for retrieval of atmospheric composition with the quadrupole mass spectrometer of the Sample Analysis at Mars instrument suite on Mars Science Laboratory. *Planetary and Space Science*, *96*, 99–113. https://doi.org/https://doi.org/10.1016/j.pss.2014.03.005

Franz, H. B., Kim, S.-T., Farquhar, J., Day, J. M. D., Economos, R. C., McKeegan, K. D., et al. (2014). Isotopic links between atmospheric chemistry and the deep sulphur cycle on Mars. *Nature*, *508*(7496), 364–368. https://doi.org/http://dx.doi.org/10.1038/nature13175

Franz, H. B., McAdam, A. C., Ming, D. W., Freissinet, C., Mahaffy, P. R., Eldridge, D. L., et al. (2017). Large sulfur isotope fractionations in Martian sediments at Gale crater. *Nature Geoscience*, *10*, 658. Retrieved from https://doi.org/10.1038/ngeo3002

Franz, H. B., Mahaffy, P. R., Webster, C. R., Flesch, G. J., Raaen, E., Freissinet, C., et al. (2020). Indigenous and exogenous organics and surface–atmosphere cycling inferred from carbon and oxygen isotopes at Gale crater. *Nature Astronomy*, *4*(5), 526–532. https://doi.org/10.1038/s41550-019-0990-x

Freissinet, C., Glavin, D. P., Buch, A., Szopa, C., Teinturier, S., Archer, P. D. J., et al. (2019). Detection of Long-Chain Hydrocarbons on Mars with the Sample Analysis at Mars (SAM) Instrument. *Ninth International Conference on Mars*. Pasadena, California: Lunar and Planetary Institute. Retrieved from http://www.lpi.usra.edu/meetings/ninthmars2019/pdf/6123.pdf

Gasda, P. J., Das, D., Nellessen, M., Dehouck, E., Rapin, W., Meslin, P.-Y., et al. (2020). Veins in Glen Torridon, Gale Crater, Mars: Exploring the Potential Transition into the Sulfate-Bearing Unit. *51st Lunar and Planetary Science Conference*, LPI Contrib. No. 1641.

Ghosh, W., & Dam, B. (2009). Biochemistry and molecular biology of lithotrophic sulfur oxidation by taxonomically and ecologically diverse bacteria and archaea. *FEMS Microbiology Reviews*, *33*(6), 999–1043. https://doi.org/10.1111/j.1574-6976.2009.00187.x

Glavin, D. P., Freissinet, C., Miller, K. E., Eigenbrode, J. L., Brunner, A. E., Buch, A., et al. (2013). Evidence for perchlorates and the origin of chlorinated hydrocarbons detected by SAM at the Rocknest aeolian deposit in Gale Crater. *Journal of Geophysical Research: Planets*, *118*(10), 1955–1973. https://doi.org/10.1002/jgre.20144

Grotzinger, J. P., & Milliken, R. E. (2012). The Sedimentary Rock Record of Mars: Distribution, Origins, and Global Stratigraphy. In J. P. Grotzinger & R. E. Milliken (Eds.), *Sedimentary Geology of Mars* (Vol. 102, pp. 1–48). SEPM Society for Sedimentary Geology. https://doi.org/10.2110/pec.12.102.0001

Grotzinger, J. P., Crisp, J., Vasavada, A. R., Anderson, R. C., Baker, C. J., Barry, R., et al. (2012). Mars Science Laboratory Mission and Science Investigation. *Space Science Reviews*, *170*, 5–56. https://doi.org/10.1007/s11214-012-9892-2

Grotzinger, J. P., Crisp, J. A., Vasavada, A. R., & the MSL Science Team. (2015). Curiosity's Mission of Exploration at Gale Crater, Mars. *Elements*, *11*, 19–26. https://doi.org/10.2113/gselements.11.1.19

Hyde, B. C., King, P. L., Dyar, M. D., Spilde, M. N., & Ali, A.-M. S. (2011). Methods to analyze metastable and microparticulate hydrated and hydrous iron sulfate minerals. *American Mineralogist*, *96*(11-12), 1856–1869. https://doi.org/10.2138/am.2011.3792

This article is protected by copyright. All rights reserved.

Accepted Article

Keil, R. G., & Mayer, L. M. (2013). *Mineral Matrices and Organic Matter*. *Treatise on Geochemistry: Second Edition* (2nd ed., Vol. 12). Elsevier Ltd. https://doi.org/10.1016/B978-0-08-095975-7.01024-X

King, P. L., & McLennan, S. M. (2010). Sulfur on Mars. *Elements*, *6*(2), 107–112. https://doi.org/10.2113/gselements.6.2.107

King, P. L., & McSween Jr., H. Y. (2005). Effects of H2O, pH, and oxidation state on the stability of Fe minerals on Mars. *Journal of Geophysical Research: Planets*, *110*(E12). https://doi.org/https://doi.org/10.1029/2005JE002482

King, P. L., Wheeler, V. M., Renggli, C. J., Palm, A. B., Wilson, S. A., Harrison, A. L., et al. (2018). Gas–Solid Reactions: Theory, Experiments and Case Studies Relevant to Earth and Planetary Processes. *Reviews in Mineralogy and Geochemistry*, *84*(1), 1–56. https://doi.org/10.2138/rmg.2018.84.1

Kloprogge, J. T., Ding, Z., Martens, W. N., Schuiling, R. D., Duong, L. V, & Frost, R. L. (2004). Thermal decomposition of syngenite, K2Ca(SO4)2·H2O. *Thermochimica Acta*, *417*(1), 143–155. https://doi.org/https://doi.org/10.1016/j.tca.2003.12.001

Kronyak, R. E., Kah, L. C., Edgett, K. S., VanBommel, S. J., Thompson, L. M., Wiens, R. C., et al. (2019). Mineral-Filled Fractures as Indicators of Multigenerational Fluid Flow in the Pahrump Hills Member of the Murray Formation, Gale Crater, Mars. *Earth and Space Science*, *6*(2), 238–265. https://doi.org/10.1029/2018EA000482

Kusakabe, M., Komoda, Y., Takano, B., & Abiko, T. (2000). Sulfur isotopic effects in the disproportionation reaction of sulfur dioxide in hydrothermal fluids: implications for the δ34S variations of dissolved bisulfate and elemental sulfur from active crater lakes. *Journal of Volcanology and Geothermal Research*, *97*(1), 287–307. https://doi.org/https://doi.org/10.1016/S0377-0273(99)00161-4

Lasne, J., Noblet, A., Szopa, C., Navarro-González, R., Cabane, M., Poch, O., et al. (2016). Oxidants at the surface of Mars: A review in light of recent exploration results. *Astrobiology*, *16*, 977–996.

Leshin, L. A., Mahaffy, P. R., Webster, C. R., Cabane, M., Coll, P., Conrad, P. G., et al. (2013). Volatile, isotope, and organic analysis of martian fines with the Mars Curiosity rover. *Science*, *341*(6153). https://doi.org/10.1126/science.1238937

Lewis, J. M. T., Watson, J. S., Najorka, J., Luong, D., & Sephton, M. A. (2015). Sulfate minerals: a problem for the detection of organic compounds on Mars? *Astrobiology*, *15*(3), 247–58. https://doi.org/10.1089/ast.2014.1160

Lewis, J. M. T., Eigenbrode, J. L., Wong, G. M., McAdam, A. C., Archer, P. D., Sutter, B., et al. (2021). Pyrolysis of Oxalate, Acetate, and Perchlorate Mixtures and the Implications for Organic Salts on Mars. *Journal of Geophysical Research: Planets*, *126*(4), e2020JE006803. https://doi.org/https://doi.org/10.1029/2020JE006803

Mahaffy, P. (2013). MSL SAM Level 2 Data, MSL-M-SAM-5-RDR-L2-V1.0. NASA Planetary Data System. Retrieved from https://doi.org/10.17189/1519510

Mahaffy, P. R., Webster, C. R., Cabane, M., Conrad, P. G., Coll, P., Atreya, S. K., et al. (2012). The sample analysis at Mars investigation and instrument suite. *Space Science Reviews*, *170*(1-4), 401–478. https://doi.org/10.1007/s11214-012-9879-z

Matsuzaki, R., Masumizu, H., Murakami, N., & Saeki, Y. (1978). The Thermal Decomposition Process of Calcium Sulfite. *Bulletin of the Chemical Society of Japan*, *51*(1), 121–122. https://doi.org/10.1246/bcsj.51.121

McAdam, A. C., Sutter, B., Archer, P. D., Franz, H. B., Eigenbrode, J. L., Knudson, C. A., et al.

This article is protected by copyright. All rights reserved.

(submitted). Evolved gas analyses of sedimentary rocks from the Glen Torridon Clay-Bearing Unit, Gale crater, Mars: Results from the Mars Science Laboratory Sample Analysis at Mars Instrument Suite.

McAdam, A. C., Franz, H. B., Sutter, B., Archer Jr, P. D., Freissinet, C., Eigenbrode, J. L., et al. (2014). Sulfur-bearing phases detected by evolved gas analysis of the Rocknest aeolian deposit, Gale Crater, Mars. *Journal of Geophysical Research: Planets*, *119*, 373–393. https://doi.org/10.1002/2013JE004518.Received

McAdam, A. C., Knudson, C. A., Sutter, B., Franz, H. B., Archer Jr., P. D., Eigenbrode, J. L., et al. (2016). Reactions Involving Calcium and Magnesium Sulfates as Potential Sources of Sulfur Dioxide During MSL SAM Evolved Gas Analyses. *47th Lunar and Planetary Science Conference (2016)*.

McAdam, A. C., Sutter, B., Archer, P. D., Franz, H. B., Wong, G. M., Lewis, J. M. T., et al. (2020). Constraints on the Mineralogy and Geochemistry of the Vera Rubin ridge, Gale crater, Mars, from Mars Science Laboratory Sample Analysis at Mars Evolved Gas Analyses. *Journal of Geophysical Research: Planets*, *125*(11), e2019JE006309. https://doi.org/10.1029/2019JE006309

McAdam, A. C., Sutter, B., Archer, P. D., Franz, H. B., Eigenbrode, J. L., Knudson, C. A., et al. (2021). Investigation of the Glen Torridon Clay-Bearing Unit and Overlying Greenheugh Pediment by the Sample Analysis at Mars Instrument Suite. *52nd Lunar and Planetary Science Conference*, LPI Contrib. No. 2548.

Millan, M., Williams, A. J., McAdam, A. C., Eigenbrode, J. L., Freissinet, C., Glavin, D. P., et al. (submitted). Organic Molecules Detected in Glen Torridon, Gale crater, Mars, by the SAM instrument aboard Curiosity.

Milliken, R. E., Grotzinger, J. P., & Thomson, B. J. (2010). Paleoclimate of Mars as captured by the stratigraphic record in Gale Crater. *Geophysical Research Letters*, *37*(4). https://doi.org/10.1029/2009GL041870

Ming, D. W., Archer Jr., P. D., Glavin, D. P., Eigenbrode, J. L., Franz, H. B., Sutter, B., et al. (2014). Volatile and Organic Compositions of Sedimentary Rocks in Yellowknife. *Science*, *343*(6169), 1245267–1–9. https://doi.org/10.1126/science.1245267

Morrison, S. M., Downs, R. T., Blake, D. F., Vaniman, D. T., Ming, D. W., Hazen, R. M., et al. (2018). Crystal chemistry of martian minerals from Bradbury Landing through Naukluft Plateau, Gale crater, Mars. *American Mineralogist*, *103*(6), 857–871. https://doi.org/10.2138/am-2018-6124

Muyzer, G., & Stams, A. J. M. (2008). The ecology and biotechnology of sulphate-reducing bacteria. *Nature Reviews. Microbiology*, *6*(6), 441–454. https://doi.org/http://dx.doi.org/10.1038/nrmicro1892

O'Connell-Cooper, C. D., Gellert, R., & Thompson, L. M. (submitted). APXS-derived chemistry of the clay-bearing Glen Torridon region of Gale crater, Mars.

Percak- Dennett, E., He, S., Converse, B., Konishi, H., Xu, H., Corcoran, A., et al. (2017). Microbial acceleration of aerobic pyrite oxidation at circumneutral pH. *Geobiology*, *15*(5), 690–703. https://doi.org/10.1111/gbi.12241

Pryor, W. A. (1960). The Kinetics of the Disproportionation of Sodium Thiosulfate to Sodium Sulfide and Sulfate. *Journal of the American Chemical Society*, *82*(18), 4794–4797. https://doi.org/10.1021/ja01503a010

Quinn, R. C., Chittenden, J. D., Kounaves, S. P., & Hecht, M. H. (2011). The oxidation-reduction potential of aqueous soil solutions at the Mars Phoenix landing site. *Geophysical*

This article is protected by copyright. All rights reserved.

Research Letters, *38*.
Rampe, E. B., Blake, D. F., Bristow, T. F., Ming, D. W., Vaniman, D. T., Morris, R. V., et al. (2020). Mineralogy and geochemistry of sedimentary rocks and eolian sediments in Gale crater, Mars: A review after six Earth years of exploration with Curiosity. *Geochemistry*, *80*(2), 125605. https://doi.org/https://doi.org/10.1016/j.chemer.2020.125605
Rogan, B., Lemke, M., Levandowsky, M., & Gorrell, T. (2005). Exploring the Sulfur Nutrient Cycle Using the Winogradsky Column. *The American Biology Teacher*, *67*(6), 348–356. https://doi.org/10.1662/0002-7685(2005)067[0348:ETSNCU]2.0.CO;2
Smith, R. J., McLennan, S. M., Sutter, B., Rampe, E. B., Dehouck, E., Siebach, K. L., et al. X-ray amorphous sulfur-bearing phases in sedimentary rocks of Gale crater, Mars. *Journal of Geophysical Research: Planets*. https://doi.org/ 10.1029/2021JE007128
Smith, R. J., McLennan, S. M., Achilles, C. N., Dehouck, E., Horgan, B. H. N., Mangold, N., et al. (2021). X-Ray Amorphous Components in Sedimentary Rocks of Gale Crater, Mars: Evidence for Ancient Formation and Long-Lived Aqueous Activity. *Journal of Geophysical Research: Planets*, *126*(3), e2020JE006782. https://doi.org/https://doi.org/10.1029/2020JE006782
Stern, J. C., Sutter, B., Archer, P. D., Eigenbrode, J. L., McAdam, A. C., Franz, H. B., et al. (2018). Major Volatiles Evolved From Eolian Materials in Gale Crater. *Geophysical Research Letters*, *45*(19), 10,240–10,248. https://doi.org/10.1029/2018GL079059
Summons, R. E., Amend, J. P., Bish, D., Buick, R., Cody, G. D., Des Marais, D. J., et al. (2011). Preservation of Martian Organic and Environmental Records: Final Report of the Mars Biosignature Working Group. *Astrobiology*, *11*(2), 157–181. https://doi.org/10.1089/ast.2010.0506
Sutter, B., McAdam, A. C., Mahaffy, P. R., Ming, D. W., Edgett, K. S., Rampe, E. B., et al. (2017). Evolved gas analyses of sedimentary rocks and eolian sediment in Gale Crater, Mars: Results of the Curiosity rover's sample analysis at Mars instrument from Yellowknife Bay to the Namib Dune. *Journal of Geophysical Research: Planets*, *122*(12), 2574–2609. https://doi.org/10.1002/2016JE005225
Thorpe, M. T., Bristow, T. F., Rampe, E. B., Tosca, N. J., Grotzinger, J. P., Fedo, C. M., & Chipera, S. J. (submitted). The Mineralogy and Sedimentary History of the Glen Torridon Region, as detailed by the Mars Science Laboratory CheMin Instrument.
Vaniman, D. T., Bish, D. L., Ming, D. W., Bristow, T. F., Morris, R. V, Blake, D. F., et al. (2014). Mineralogy of a Mudstone at Yellowknife Bay, Gale Crater, Mars. *Science*, *343*(6169), 1243480.
Vaniman, D. T., Martínez, G. M., Rampe, E. B., Bristow, T. F., Blake, D. F., Yen, A. S., et al. (2018). Gypsum, bassanite, and anhydrite at Gale crater, Mars. *American Mineralogist*, *103*(7), 1011–1020. https://doi.org/10.2138/am-2018-6346
Webster, C. R., Mahaffy, P. R., Flesch, G. J., Niles, P. B., Jones, J. H., Leshin, L. A., et al. (2013). Isotope Ratios of H, C, and O in CO2 and H2O of the Martian Atmosphere. *Science*, *341*(6143), 260 LP – 263. https://doi.org/10.1126/science.1237961
Wong, G. (2020). Processed data for figures and analysis in "Detection of reduced sulfur on Vera Rubin ridge by quadratic discriminant analysis of volatiles observed during evolved gas analysis." Harvard Dataverse. https://doi.org/doi:10.7910/DVN/UOURYF
Wong, G. (2022). Processed data for figures and analysis in "Oxidized and reduced sulfur observed by the Sample Analysis at Mars (SAM) instrument suite on the Curiosity rover within the Glen Torridon region at Gale crater, Mars." Harvard Dataverse.

This article is protected by copyright. All rights reserved.

https://doi.org/doi:10.7910/DVN/LYUT1S
Wong, G. M., Lewis, J. M. T., Knudson, C. A., Millan, M., McAdam, A. C., Eigenbrode, J. L., et al. (2020). Detection of reduced sulfur on Vera Rubin ridge by quadratic discriminant analysis of volatiles observed during evolved gas analysis. *Journal of Geophysical Research: Planets*, *125*(8). https://doi.org/10.1029/2019JE006304
Wray, J. J. (2013). Gale crater: the Mars Science Laboratory / Curiosity Rover Landing Site. *International Journal of Astrobiology*, *12*(1), 25–38. https://doi.org/10.1017/S1473550412000328

References From the Supporting Information

Archer Jr., P. D., Franz, H. B., Sutter, B., Arevalo Jr, R. D., Coll, P., Eigenbrode, J. L., et al. (2014). Abundances and implications of volatile-bearing species from evolved gas analysis of the Rocknest aeolian deposit, Gale Crater, Mars. *Journal of Geophysical Research: Planets*, *119*, 237–254. https://doi.org/10.1002/2013JE004493
Driscoll, R. L., & Leinz, R. W. (2005). *Methods for Synthesis of Some Jarosites: U.S. Geological Survey Techniques and Methods 5-D1*. Reston, VA.
Feng, T., Zhou, P., Zhao, X., Li, L., Xia, X., Zhang, S., et al. (2019). Sulfur Evolution Reaction during Reduction of SO2 with CO over Carbon Materials. *Energy & Fuels*, *33*(8), 7491–7499. https://doi.org/10.1021/acs.energyfuels.9b00748
Frigge, L., Elserafi, G., Ströhle, J., & Epple, B. (2016). Sulfur and Chlorine Gas Species Formation during Coal Pyrolysis in Nitrogen and Carbon Dioxide Atmosphere. *Energy & Fuels*, *30*(9), 7713–7720. https://doi.org/10.1021/acs.energyfuels.6b01080
Glavin, D. P., Freissinet, C., Miller, K. E., Eigenbrode, J. L., Brunner, A. E., Buch, A., et al. (2013). Evidence for perchlorates and the origin of chlorinated hydrocarbons detected by SAM at the Rocknest aeolian deposit in Gale Crater. *Journal of Geophysical Research: Planets*, *118*(10), 1955–1973. https://doi.org/10.1002/jgre.20144
Lewis, J. M. T., Eigenbrode, J. L., Wong, G. M., McAdam, A. C., Archer, P. D., Sutter, B., et al. (2021). Pyrolysis of Oxalate, Acetate, and Perchlorate Mixtures and the Implications for Organic Salts on Mars. *Journal of Geophysical Research: Planets*, *126*(4), e2020JE006803. https://doi.org/https://doi.org/10.1029/2020JE006803
McAdam, A. C., Franz, H. B., Sutter, B., Archer Jr, P. D., Freissinet, C., Eigenbrode, J. L., et al. (2014). Sulfur-bearing phases detected by evolved gas analysis of the Rocknest aeolian deposit, Gale Crater, Mars. *Journal of Geophysical Research: Planets*, *119*, 373–393. https://doi.org/10.1002/2013JE004518.
Shao, D., Hutchinson, E. J., Heidbrink, J., Pan, W.-P., & Chou, C.-L. (1994). Behavior of sulfur during coal pyrolysis. *Journal of Analytical and Applied Pyrolysis*, *30*(1), 91–100. https://doi.org/https://doi.org/10.1016/0165-2370(94)00807-8
Wong, G. (2020). Processed data for figures and analysis in "Detection of reduced sulfur on Vera Rubin ridge by quadratic discriminant analysis of volatiles observed during evolved gas analysis." Harvard Dataverse. https://doi.org/doi:10.7910/DVN/UOURYF
Wong, G. M., Lewis, J. M. T., Knudson, C. A., Millan, M., McAdam, A. C., Eigenbrode, J. L., et al. (2020). Detection of reduced sulfur on Vera Rubin ridge by quadratic discriminant analysis of volatiles observed during evolved gas analysis. *Journal of Geophysical Research: Planets*, *125*(8). https://doi.org/10.1029/2019JE006304

This article is protected by copyright. All rights reserved.

Accepted Article

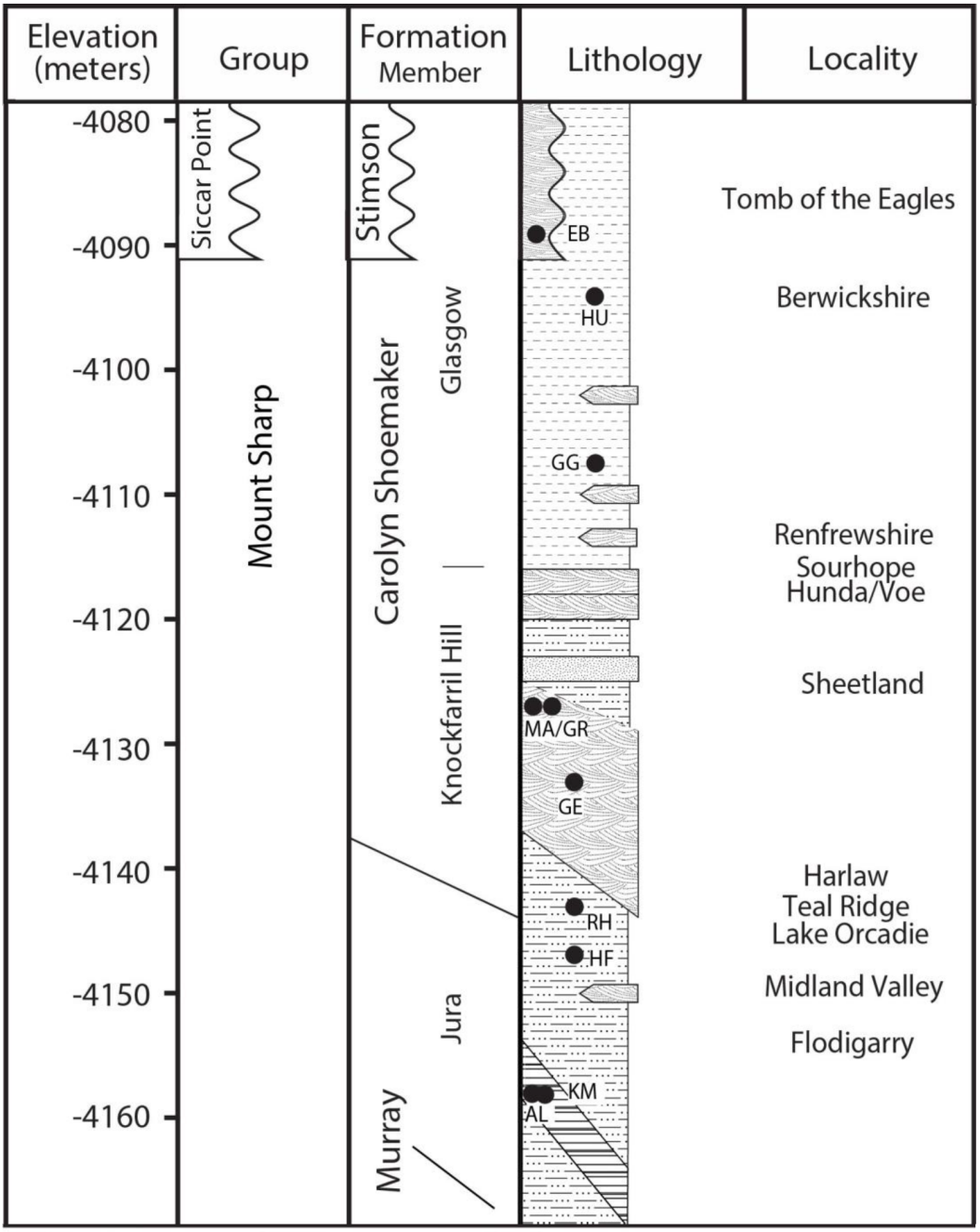

Sandstone

Cross-Stratified Pebbly Sandstone

Thinly and thickly Laminated Mudstone

Mudstone with Faint Laminations

Laminated Mudstone with minor Sandstone as Cross-Stratified Lenses

Drill Hole

AL, Aberlady KM, Kilmarie HF, Highfield RH, Rock Hall
GE, Glen Etive MA, Mary Anning GR,Groken GG, Glasgow
HU, Hutton EB, Edinburgh

This article is protected by copyright. All rights reserved.

Accepted Article

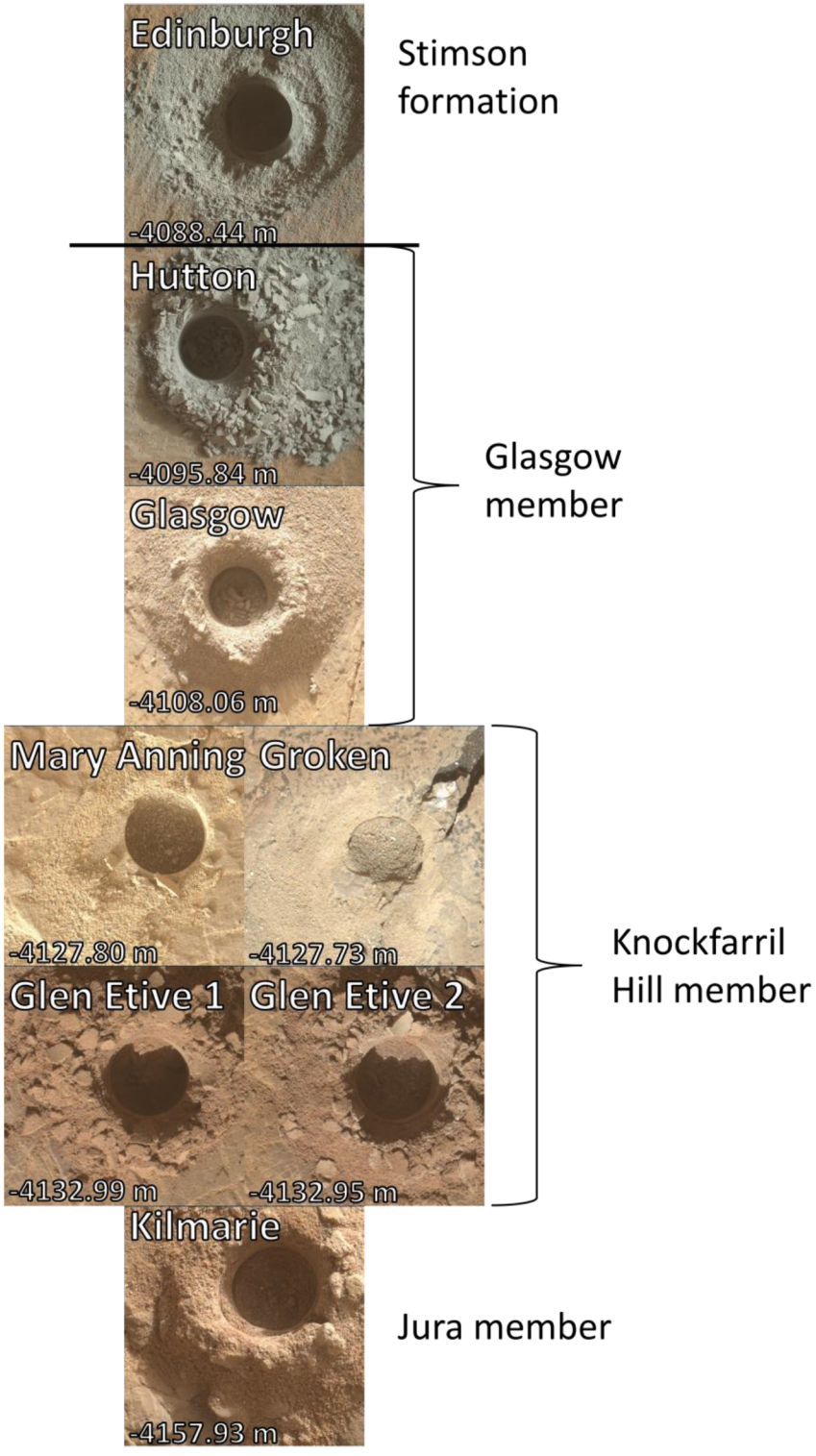

This article is protected by copyright. All rights reserved.

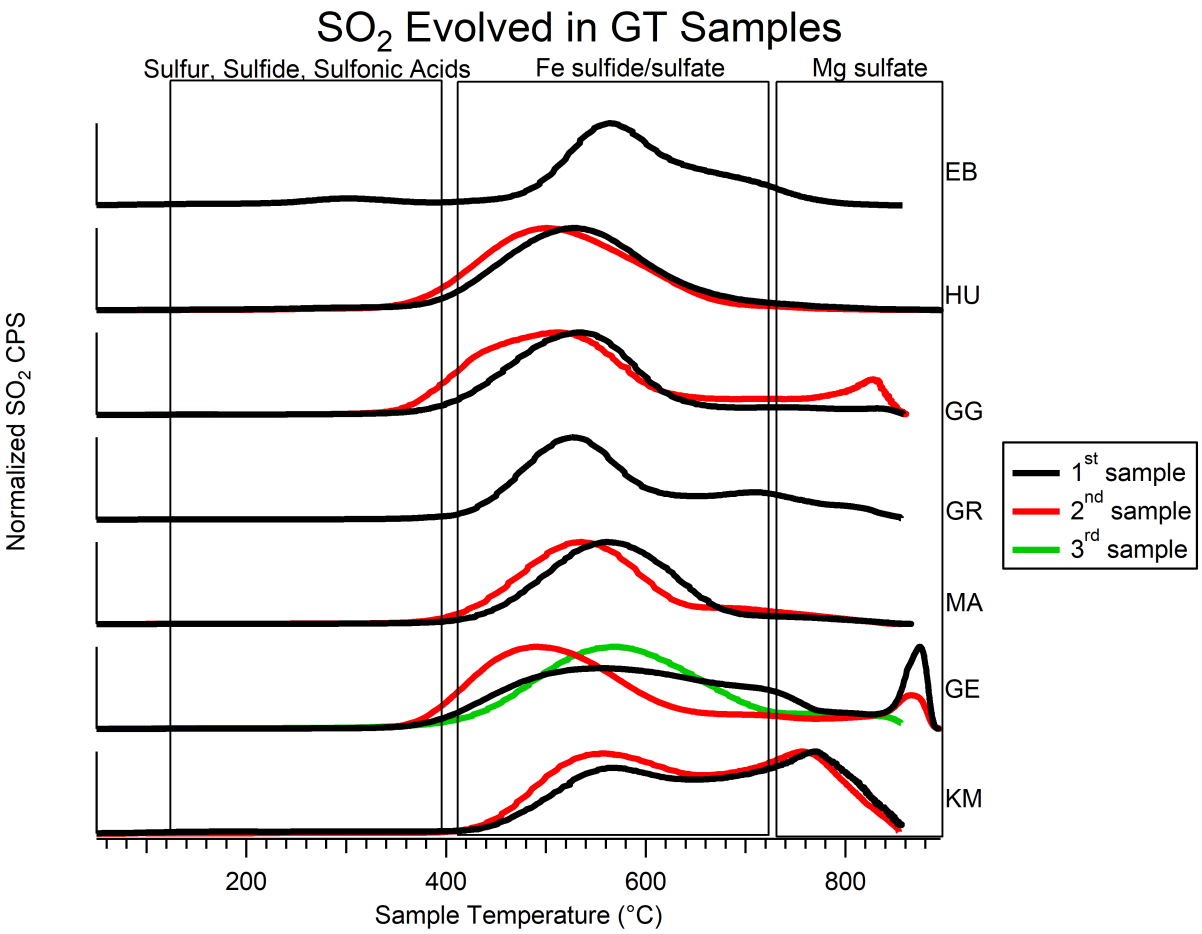

Accepted Article

This article is protected by copyright. All rights reserved.

Accepted Article

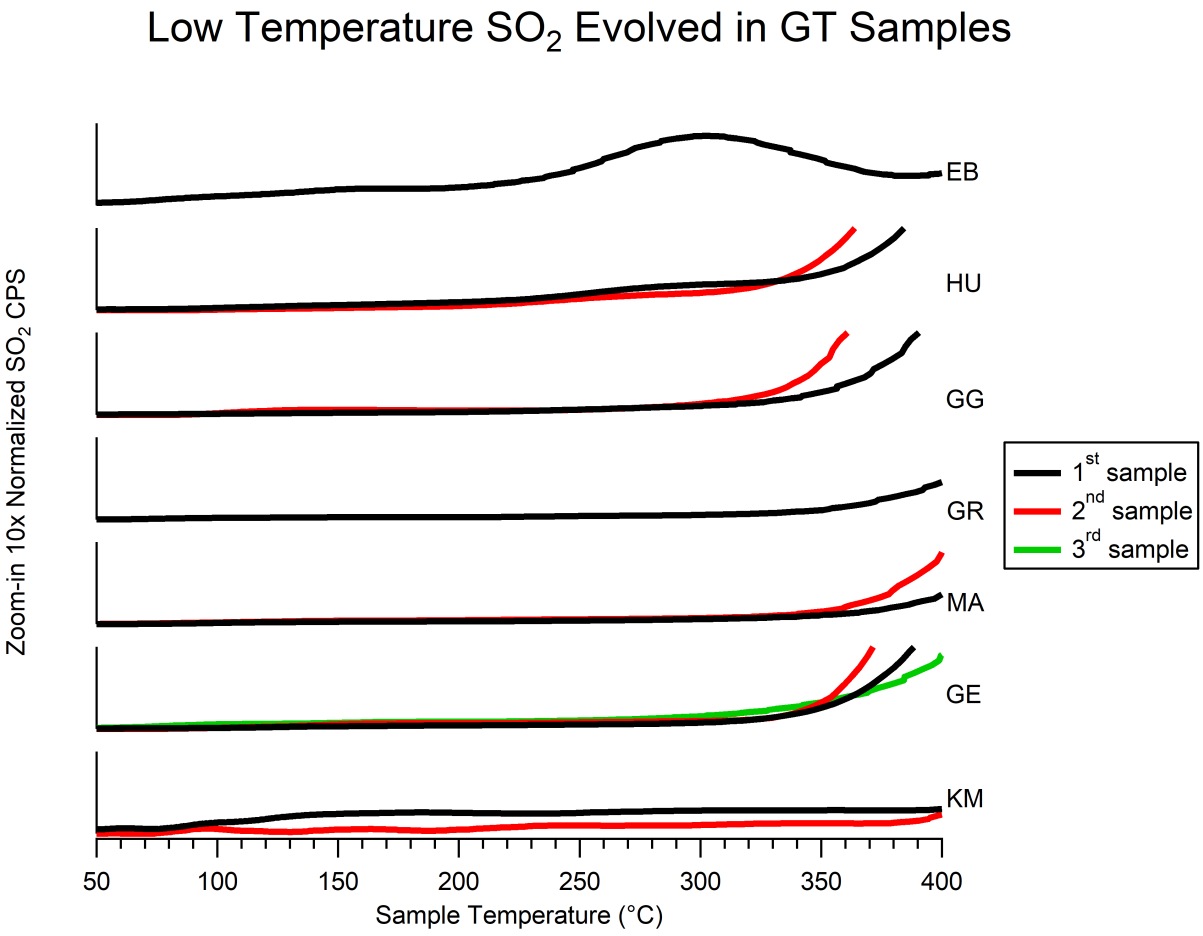

This article is protected by copyright. All rights reserved.

Accepted Article

SAMPLE	PEAK TEMP. OF IRON SULFATE/SULFIDE SO_2 RELEASE (˚C)	LOW TEMP. SO_2 RELEASE (˚C)	SULFIDE QDA POSTERIOR PROBABILITY	QMS S ISOTOPES ($\delta^{34}S$ V-CDT; ‰)
EB	562	297	73%	-27 ± 7
HU1	529	N/A	11%	18 ± 6
HU2	503	N/A	1%	21 ± 4
GG1	534	N/A	1%	5 ± 9
GG2	514	N/A	<1%	-5 ± 9
GR	526	N/A	1%	2 ± 6
MA1	563	N/A	1%	8 ± 5
MA2	538	N/A	1%	11 ± 6
GE1	555	N/A	7%	20 ± 4
GE2	490	N/A	11%	-6 ± 7
GE3	568	N/A	9%	-14 ± 5
KM1	568	N/A	97%	-21 ± 19
KM2	557	N/A	63%	0 ± 20

This article is protected by copyright. All rights reserved.